ELSEVIER

PII:S0140-7007(97)00069-8

Int J. Refrig. Vol. 21, No. 1, pp. 64–76, 1998
Published by Elsevier Science Ltd
Printed in Great Britain
0140-7007/98/$19.00+00

Thermodynamic properties of R32 + R134a and R125 + R32 mixtures in and beyond the critical region*

S.B. Kiselev and M.L. Huber
Physical and Chemical Properties Division, National Institute of Standards and Technology, 325 Broadway, Boulder , CO 80303, USA

A parametric crossover equation of state for pure fluids is adapted to binary mixtures. This equation incorporates scaling laws asymptotically close to the critical point and is transformed into a regular classical expansion far away from the critical point. An isomorphic generalization of the law of corresponding states is applied to the prediction of thermodynamic properties and the phase behavior of binary mixtures over a wide region around the locus of vapor–liquid critical points. A comparison is made with experimental data for pure R32, R125 and R134a, and for R32 + R134a and R125 + R32 binary mixtures. The equation of state yields a good representation of thermodynamic property data in the range of temperatures $0.8T_c(x) \leq T \leq 1.5T_c(x)$ and densities $0.35\rho_c(x) \leq \rho \leq 1.65\rho_c(x)$. Published by Elsevier Science Ltd.
(Keywords: binary mixtures; equation of state; R32; R125; R134a; thermodynamic properties)

Propriétés thermodynamiques des mélanges R32 + R134a et R125 + R32, dans et au déla de la région critique

One adapte une équation d'état paramétrique pour fluides purs à des mélanges binaires. Cette équation comprend des lois asymptotiques près du point critique, et est transformée en un développement classique régulier loin du point critique. On applique une généralisation isomorphique de la loi des états correspondants pour la prédiction des propriétés thermodynamiques et du comportement des phases des mélanges binaires, sur une large région autour des points critiques vapeur-liquide. On fait une comparaison avec des données expérimentales pour les fluides purs R32, R125, et R134a, et pour les mélanges binaires R32 + R134a et R125 + R32. L'équation d'état fournit une bonne réprésentation des propriétés thermodynamiques dans la gamme de températures $0.8T_c(x) \leq T \leq 1.5T_c(x)$ *et de densités* $0.35\ \rho_c(x) \leq \rho \leq 1.65\rho_c(x)$. Published by Elsevier Science Ltd.
(Mots clés: mélange binaire; équation d'état; R32; R125; R134a; propriété thermodynamique)

Introduction

Refrigerant mixtures such as R32 + R134a and R125 + R32 are of interest as candidates to replace ozone-depleting refrigerants scheduled to be phased out. Most models that are currently in use for predicting the thermophysical properties of these mixtures cannot accurately represent properties in and around the critical region. In this work we present a crossover free-energy model for R32 + R134a and R125 + R32 mixtures based on a parametric crossover equation of state[1,2] which reproduces scaling laws at the critical region and is transformed into a regular classical expansion far away from the critical point. The equation of state for binary mixtures in this model depends only on the excess critical compressibility factor, so that if the critical locus of the mixture is known, all other thermodynamic properties can be predicted. We apply this model to R32 + R134a and R125 + R32 systems, and compare with experimental data.

Crossover free-energy for binary mixtures

In accordance with the principle of critical-point universality with appropriately chosen thermodynamic variables, also called isomorphic variables, the thermodynamic potential of binary mixtures has the same form as the thermodynamic potential of a one-component fluid. In the present paper we use the same

* Contribution of the National Institute of Standards and Technology, not subject to copyright in the United States

thermodynamic variables as adopted by Kiselev and coworkers[1-3].

Let ρ be the density, T the temperature, and A the Helmholtz free-energy per mole of a pure fluid. In addition, we define two dimensionless 'distances' from the critical point

$$\tau = \frac{T - T_c}{T_c}, \quad \Delta\rho = \frac{\rho - \rho_c}{\rho_c}, \tag{1}$$

where T_c is the critical temperature and ρ_c is the critical density. The isomorphic free-energy density of a binary mixture is given by[1-3].

$$\rho\tilde{A}(T, \rho, \tilde{x}) = \rho A(T, \rho, x) - \rho\tilde{\mu}x(T, \rho, \tilde{x}), \tag{2}$$

where $\tilde{\mu} = \mu_2 - \mu_1$ is the difference between the chemical potentials μ_1 and μ_2 of the mixture components, and $x = N_2/(N_1 + N_2)$ is the mole fraction of the second component in the mixture. The isomorphic variable $\tilde{x}$ is related to the field variable ζ, first introduced by Leung and Griffiths[4] by the relation

$$\tilde{x} = 1 - \zeta = \frac{e^{\tilde{\mu}/RT}}{1 + e^{\tilde{\mu}/RT}}. \tag{3}$$

The thermodynamic equation

$$x = -\tilde{x}(1 - \tilde{x})\left(\frac{\partial\tilde{A}}{\partial\tilde{x}}\right)_{T,\rho}\frac{1}{RT} \tag{4}$$

(where R is the universal gas constant) provides a relation between the concentration x and the isomorphic variable $\tilde{x}$. At fixed $\tilde{x}$, the isomorphic free-energy $\rho\tilde{A}$ will be the same function of τ and ρ as the Helmholtz free-energy density of a one-component fluid. Based on the crossover equation of state for a pure fluid[1-3], the isomorphic free-energy density of binary mixtures reads

$$\begin{aligned}\frac{\rho\tilde{A}(T, \rho, \tilde{x})}{R\rho_{c0}T_{c0}} &= \tilde{k}r^{2-\alpha}[R(q)]^{\alpha} \\ &\times \left[\tilde{a}\Psi_0(\theta) + \sum_{i=1}^{5}\tilde{c}_i r^{\Delta_i}[R(q)]^{-\tilde{\Delta}_i}\Psi_i(\theta)\right] \\ &+ \sum_{i=1}^{4}(\tilde{A}_i + \frac{\rho}{\rho_c}\tilde{m}_i)\tau^i(\tilde{x}) - \frac{P_c(\tilde{x})}{R\rho_{c0}T_{c0}} \\ &+ \frac{\rho T}{\rho_{c0}T_{c0}}\left[\ln(1 - \tilde{x}) + \tilde{m}_0\right],\end{aligned} \tag{5}$$

$$\tau = \frac{T - T_c(\tilde{x})}{T_c(\tilde{x})} = r(1 - b^2\theta^2), \tag{6}$$

$$\Delta\rho = \frac{\rho - \rho_c(\tilde{x})}{\rho_c(\tilde{x})} = \tilde{k}r^{\beta}[R(q)]^{\beta + 1/2}\theta + \tilde{d}_1\tau, \tag{7}$$

where α, β and Δ_i are universal critical exponents, b^2 is a universal linear-model parameter, $\tilde{k}$, $\tilde{d}_1$, $\tilde{a}$ and $\tilde{c}_i$ are system-dependent coefficients, while $R(q)$ and $\Psi_i(\theta)$ are universal functions. The universal scaled functions $\Psi_i(\theta)$ are the same as those in the parametric crossover model of Kiselev and Sengers[5].

$$\Psi_i(\theta) = \sum_{j=0}^{5}\alpha_{ij}\theta^j, \quad (i = 0, \ldots, 5), \tag{8}$$

while the crossover function $R(q)$ is defined by the expression[1-3]

$$R(q) = \left(1 + \frac{q^2}{1 + q}\right)^2, \tag{9}$$

where the variable q is related to the parametric variable r by

$$q = (rg)^{1/2} \tag{10}$$

where g is the inverse rescaled Ginzburg number.

In eqns (1)–(10), all system-dependent parameters as well as the critical parameters $T_c(\tilde{x})$, $\rho_c(\tilde{x})$ and $P_c(\tilde{x})$ are analytical functions of the isomorphic variable $\tilde{x}$. For these functions we use the same expressions as Kiselev *et al.*[1-3].

$$T_c(\tilde{x}) = T_{c0}(1 - \tilde{x}) + T_{c1}\tilde{x} + \tilde{x}(1 - \tilde{x})\sum_{i=0}^{3}T_i(1 - 2\tilde{x})^i, \tag{11}$$

$$\rho_c(\tilde{x}) = \rho_{c0}(1 - \tilde{x}) + \rho_{c1}\tilde{x} + \tilde{x}(1 - \tilde{x})\sum_{i=0}^{3}\rho_i(1 - 2\tilde{x})^i, \tag{12}$$

$$P_c(\tilde{x}) = P_{c0}(1 - \tilde{x}) + P_{c1}\tilde{x} + \tilde{x}(1 - \tilde{x})\sum_{i=0}^{2}P_i(1 - 2\tilde{x})^i, \tag{13}$$

where subscripts '$c0$' and '$c1$' correspond to the first and second components of the mixture, respectively. In addition to eqns (11)–(13), we also adopt a critical line condition of the form[1-3]

$$\frac{d\tilde{m}_0}{d\tilde{x}} = \frac{1}{R\rho_c T_c}\frac{dP_c}{d\tilde{x}} + \frac{\rho_{c0}}{\rho_c}(\tilde{A}_1 + \tilde{m}_1)\frac{T_{c0}}{T_c^2}\frac{dT_c}{d\tilde{x}}, \tag{14}$$

$$T_c(\tilde{x}) = T_c(x), \quad \rho_c(\tilde{x}) = \rho_c(x), \quad P_c(\tilde{x}) = P_c(x) \tag{15}$$

The critical line condition implies that the zero of the chemical potential of a binary mixture can be chosen so that the isomorphic variable $\tilde{x} = x$ along the whole critical line, including the one-component limits.

To specify the crossover equation for $\tilde{A}(T, \rho, \tilde{x})$ of a binary mixture, we also need the system-dependent parameters $\tilde{d}_1(\tilde{x})$, $\tilde{k}(\tilde{x})$, $\tilde{a}(\tilde{x})$, $\tilde{c}_i(\tilde{x})$, $\tilde{g}(\tilde{x})$, $\tilde{m}_i(\tilde{x})$ and $\tilde{A}_i(\tilde{x})$ as functions of the isomorphic variable $\tilde{x}$. To represent all these system-dependent parameters in eqns (5)–(7), designated as $\tilde{k}_i(\tilde{x})$, as functions of $\tilde{x}$, we used an isomorphic generalization of the law of corresponding states[1,2]. The isomorphic generalization of the law of corresponding states embodies the hypothesis that all system-dependent parameters depend on $\tilde{x}$ only through the excess critical compressibility function $\Delta Z_c(\tilde{x})$, where

$$\Delta Z_c(\tilde{x}) = Z_c(\tilde{x}) - Z_{cid}(\tilde{x}) \tag{16}$$

is the difference between the actual compressibility factor of a mixture $Z_c(\tilde{x}) = P_c(\tilde{x})/R\rho_c(\tilde{x})T_c(\tilde{x})$ and its 'ideal' part $Z_{cid}(\tilde{x}) = Z_{c0}(1 - \tilde{x}) + Z_{c1}\tilde{x}$. The dimensionless

Table 1 Universal constants
Tableau 1 *Constantes universelles*

$\alpha = 0.110$
$\beta = 0.325$
$\gamma = 2 - \alpha - 2\beta = 1.24$
$b^2 = (\gamma - 2\beta)/\gamma\,(1 - 2\beta) = 1.359$
$\Delta_1 = \tilde{\Delta}_1 = 0.51$
$\Delta_2 = \tilde{\Delta}_2 = 2\,\Delta_1 = 1.02$
$\Delta_3 = \Delta_4 = \gamma + \beta - 1 = 0.565$
$\Delta_5 = 1.19$
$\tilde{\Delta}_3 = \tilde{\Delta}_4 = \Delta_3 - 1/2 = 0.065$
$\tilde{\Delta}_5 = \Delta_5 - 1/2 = 0.69$
$e = 2\gamma + 3\beta - 1$
$e_1 = (5 - 2e)(e - \beta)(3 - 2e)/3(5\beta - e)$
$e_2 = (5 - 2e)(e - 3\beta)/3(5\beta - e)$
$e_3 = 2 - \alpha - \Delta_5$
$e_4 = (5 - 2e_3)(e_3 - 3\beta)/3(5\beta - e_3)$

Table 2 Universal scaled functions
Tableau 2 *Fonction avec échelle universelle*

$\Psi_0(\theta) = (1/2b^4)[2\beta\,(b^2 - 1)/(2 - \alpha) + 2\beta\,(2\gamma - 1)$
$(1 - b^2\theta^2)/(\gamma(1 - \alpha)) + (2\beta - 1)(1 - b^2\theta^2)^2/\alpha]$
$\Psi_1(\theta) = [1/(2b^2(1 - \alpha + \Delta_1))][(\gamma + \Delta_1)/$
$(2 - \alpha + \Delta_1) - (1 - 2\beta)b^2\theta^2]$
$\Psi_2(\theta) = [1/(2b^2(1 - \alpha + \Delta_2))][(\gamma + \Delta_2)/$
$(2 - \alpha + \Delta_2) - (1 - 2\beta)b^2\theta^2]$
$\Psi_3(\theta) = \theta - (2/3)(e - \beta)b^2\theta^3 + e_1(1 - 2\beta)b^4\theta^5/(5 - 2e)$
$\Psi_4(\theta) = (1/3)b^2\theta^3 + e_2(1 - 2\beta)b^4\theta^5/(5 - 2e)$
$\Psi_5(\theta) = (1/3)b^2\theta^3 + e_4(1 - 2\beta)b^4\theta^5/(5 - 2e_3)$

Table 3 Law of corresponding states constants
Tableau 3 *Constantes pour loi des états correspondants*

	$k_i^{(1)}$
Critical amplitudes	
k	− 3.4826
d_1	-6.7567×10^{-1}
a	-2.3130×10
c_1	-3.3449×10
c_2	0
c_3	− 1.1514
c_4	2.1111×10
c_5	0
Crossover parameter	
g	9.8900
Background coefficients	
A_1	9.0968
A_2	-3.3379×10
A_3	0
$\Delta m_1 = m_{11} - m_{10}$	− 1.8073
m_1	3.1238
m_2	1.7328×10
m_3	− 5.9960

coefficients $\tilde{k}$, $\tilde{g}$, and $\tilde{d}_1$ are written in the form

$$\tilde{k}_i(\tilde{x}) = k_{i0} + (k_{i1} - k_{i0})\tilde{x} + k_i^{(1)}\Delta Z_c(\tilde{x}), \tag{17}$$

and all others coefficients are given by

$$\tilde{k}_i(\tilde{x}) = \frac{P_c(\tilde{x})}{R\rho_{c0}T_{c0}}[k_{i0} + (k_{i1} - k_{i0})\tilde{x} + k_i^{(1)}\Delta Z_c(\tilde{x})]. \tag{18}$$

In the context of the law of corresponding states, the mixing coefficients $k_i^{(1)}$ in eqns (17) and (18) are universal constants for all binary mixtures of simple fluids. For mixtures with $\Delta Z_c > 0.06$ one needs to use an extended version of the law of corresponding states with additional terms quadratic in $\Delta Z_c(\tilde{x})^2$. However, since for mixtures R32 + R134a and R125 + R32, $\Delta Z_c \ll 0.06$, we use expressions linear in $\Delta Z_c(\tilde{x})$. In the present paper, for the mixing coefficients $k_i^{(1)}$, we adopt the same values as employed earlier by Kiselev for methane + ethane and ethane + *n*-butane mixtures[1]. Our parametric crossover model for binary mixtures is specified by eqns (2)–(18), and contains the following universal constants: the critical exponents α, β, Δ_i, $\tilde{\Delta}_i$, and the linear-model parameter b^2. The values of all universal constants are listed in *Table 1*, and the universal scaled functions $\Psi_i(\theta)$ are summarized explicitly in *Table 2*. The values of the coefficients $k_i^{(1)}$ are listed in *Table 3*. The relevant thermodynamic derivatives of the crossover free-energy are summarized in Appendix A.

Crossover free-energy equation of state for pure components

In order to use the parametric crossover model defined by eqns (5)–(7), it is necessary to have the critical parameters T_c, ρ_c, and P_c. For R32 and R125, we used values by Outcalt and McLinden[6], while for R134a we use the values from[7]. We then fit experimental *PVT* data, only in the range of temperatures and densities bounded by

$$\tau + 1.2\Delta\rho^2 \leq 0.5,\ T \geq 0.995T_c \tag{19}$$

in order to obtain the fluid-specific critical amplitudes (the rescaled asymptotic critical amplitude k, the rectilinear diameter amplitude d_1 of the coexistence curve, the amplitude a of the asymptotic term, and amplitudes c_i ($i = 1,\ldots,5$) of the nonasymptotic terms, the inverse rescaled Ginzburg number g), and background coefficients A_i. We also used in the fit two additional *PVT* data points for every substance, at subcritical conditions approximately at temperatures $T = 0.9\,T_c$ and $T = 0.85\,T_c$. The coefficients resulting from the fit are given in *Table 4*. For R32 the *PVT* data were taken from references[8–11], for R125[12–16], and for R134a we used references[17–21]. *Figures 1–3* show the percentage deviations of the experimental pressures from the calculated values as a function of temperature and density for R32, R125 and R134a. Inside the region specified by eqn (19), the deviations are within 0.3%, and increase to 0.5–0.6% at the boundary. The pressure deviations for R134a correspond approximately to those found by Sengers *et al.*[7,22].

In addition, the coefficients $\tilde{m}_i$ are found from caloric data. The coefficients $\tilde{m}_0$ and $\tilde{m}_1$ determine the zero points of entropy and internal energy and may be arbitrarily set. We set both of these parameters to zero. The coefficients m_i for $i \geq 2$ determine the background contributions to the isochoric specific heat and can be

Table 4 System-dependent constants for R32, R125 and R134a

Tableau 4 *Constantes relatives au système pour R32, R125 et R134*

	R32	R125	R134a
Critical parameters			
T_c (/K)	351.350	339.330	374.274
P_c (/MPa)	5.795	3.629	4.065
ρ_c (/(mol L^{-1}))	8.208	4.760	5.050
Critical amplitudes			
k	1.3056	1.2805	1.2966
d_1	-4.8317×10^{-1}	-9.9847×10^{-1}	-9.0132×10^{-1}
a	2.2351×10	2.4831×10	2.4595×10
c_1	-6.6650	-5.7746	-5.0158
c_2	1.0082×10	5.7325	4.8422
c_3	-4.9917	-1.1853×10	-1.3199×10
c_4	3.6051	1.1422×10	1.4483×10
c_5	-1.6091	5.5508×10^{-1}	-8.0754×10^{-1}
Crossover parameter			
g	1.3573×10^{-1}	5.0000×10^{-2}	6.0000×10^{-5}
Background coefficients			
A_1	-7.4464	-7.4429	-7.6768
A_2	1.9214×10	2.3018×10	2.1123×10
A_3	-1.1567	2.8076	2.5582
m_2	-1.2406×10	-2.7824×10	-2.6675×10
m_3	-4.1327	3.0457	8.8143
Molar mass			
$g \cdot mol^{-1}$	52.02	120.02	102.03

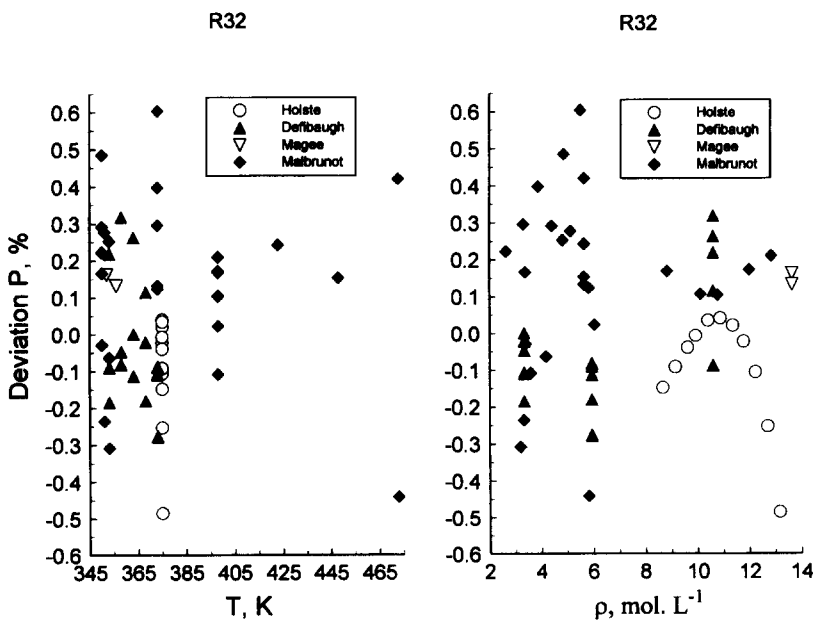

Figure 1 Percentage deviations of the experimental pressures obtained by Holste and co-workers[8], by Defibaugh and co-workers[9], by Magee[10] and by Malbrunot and co-workers[11] for R32, from values calculated with the crossover equation of state

Figure 1 *Déviations, en pourcetages, entre pressions expérimentales obtenues par Holste et al.[8], par Defibaugh et al.[9], par Magee[10] et par Malbrunot et al.[11] pour le R32, et les valeurs calculées avec l'équation d'état étendue.*

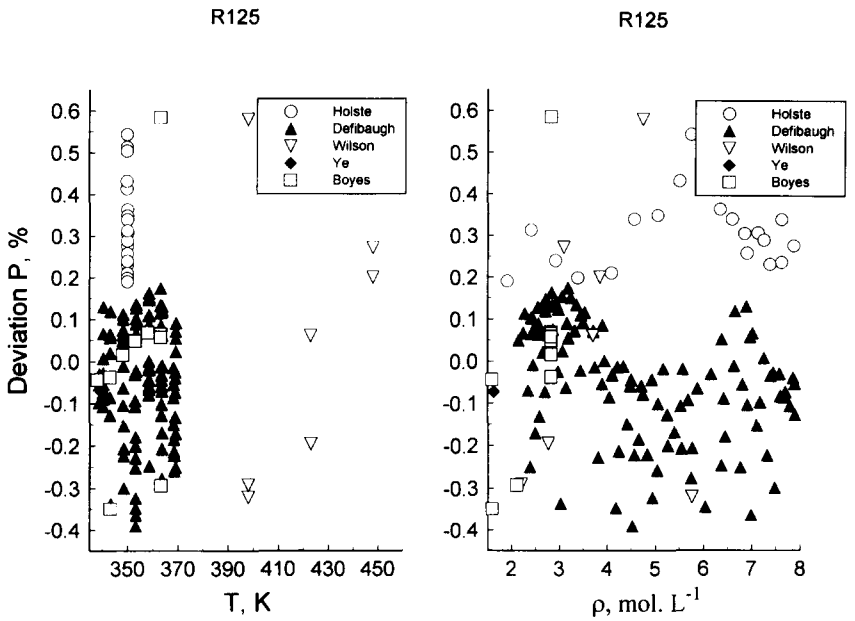

Figure 2 Percentage deviations of the experimental pressures obtained by Duarte-Garza and co-workers[12], by Defibaugh and Morrison[13], by Ye and co-workers[14], by Boyes and Weber[15] and by Wilson and co-workers[16] for R125, from values calculated with the crossover equation of state

Figure 2 *Déviations, en pourcentages, entre pressions expérimentales obtenues par Duarte-Garza et al.[12], par Defibaugh et Morrison[13], par Ye et al.[14], par Boyes et Webber[15] et par Wilson et al.[16] por le R125, et les valeurs calculées avec l'équation de l'état étendue.*

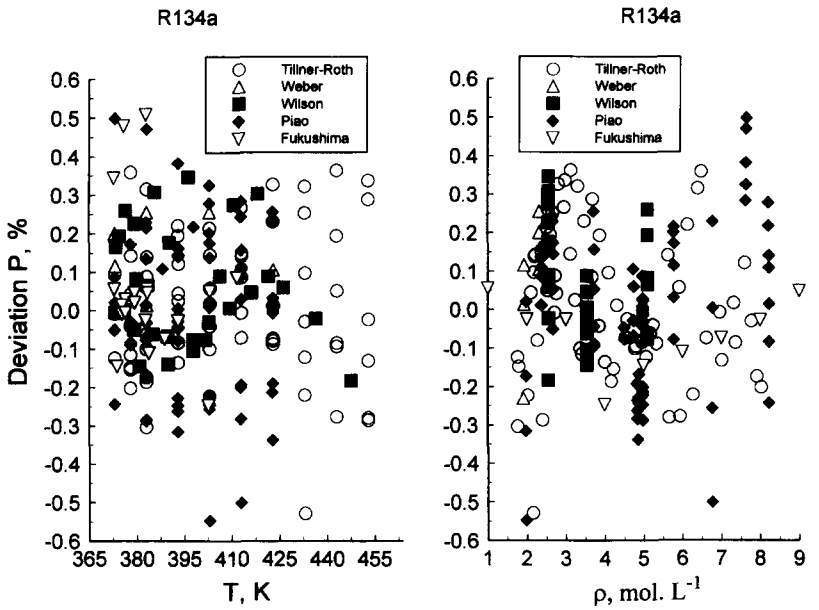

Figure 3 Percentage deviations of the experimental pressures obtained by Tillner-Roth and Baehr[17], by Weber[13], by Wilson and Basu[19], by Piao and co-workers[20] and by Fukushima[21] for R134a, from values calculated with the crossover equation of state

Figure 3 *Déviations, en pourcentages, entre pressions expérimentales obtenues par Tillner-Roth et Baehr[17], par Webber[13], par Wilson et Basu[19], par Piao et al.[20] et par Fukushima[21], et les valeurs calculées avec l'équation de l'état étendue.*

determined from fitting either heat-capacity or sound-speed data. Unfortunately, there are little sound-speed or heat-capacity data in the critical region for R32, R125 or R134a, although there are data at lower temperatures. Therefore we chose to find the coefficients m_2, m_3 and m_4 from a fit of the crossover model to sound-speed values calculated from high-accuracy equations of state for these fluids. We generated sound-speeds at near-critical isochores and temperatures $1.2T_c \leq T \leq 1.5T_c$ using the equation of state from[23] for R134a, and reference[6] for

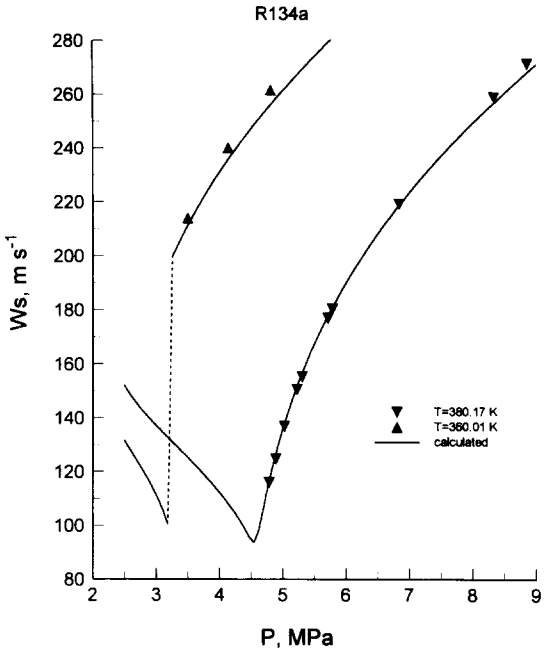

Figure 4 The sound-velocity of R134a as a function of pressure at two temperatures. The symbols indicate experimental data obtained by Guedes and Zollweg[24] and the curves represent values calculated with the crossover model

Figure 4 *Vitesse du son du R134a en fonction de la pression, à deux températures. Les symboles indiquent les données expérimentales obtenues par Guedes et Zollweg*[24] *et les courbes représentent les valeurs calculées evec le modèle étendu*

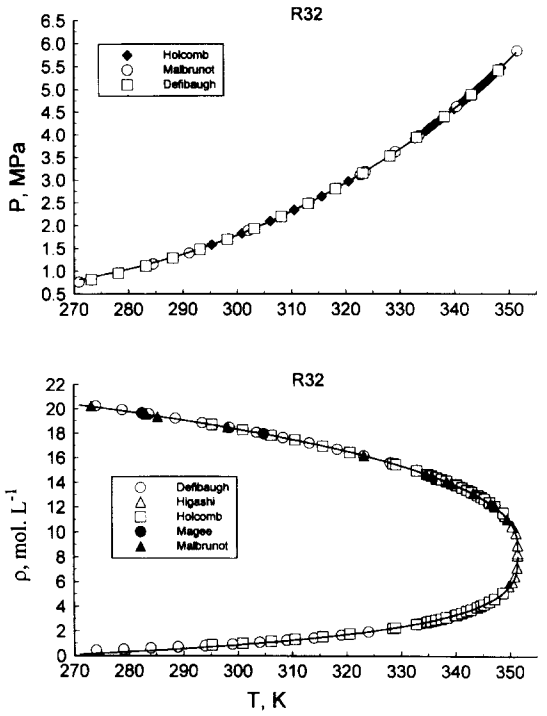

Figure 5 VLE data for R32 obtained by Holcomb and co-workers[25], by Defibaugh and co-workers[9], by Higashi[26], by Magee[10] and by Malbrunot and co-workers[11] for R32, with predictions of the crossover equation of state

Figure 5 *Données VLE du le R32, obtenues par Holcomb et al.*[25]*, par Malbrunot et al.*[11]*, par Defigaugh et al.*[9]*, par Higashi*[26]*, par Magee*[10] *et par Malbrunot et al.*[11]*, avec les prédictions de l'équation état étendue*

Table 5 Critical-line parameters for R32 + R134a and R125 + R32 mixtures

Tableau 5 *Paramètres de la ligne critique pour les mélanges R32 + R134a et R125 + R32*

Critical parameters	R32 + R134a	R125 + R32
Temperature (/K)		
T_{c0}	351.350	339.330
T_0	3.5497	-1.3295×10
T_1	-3.2169×10^{-1}	3.6711
T_2	-5.8159×10^{-1}	−2.3034
T_{cl}	374.274	351.350
Density (/(mol L^{-1}))		
ρ_{c0}	8.208	4.760
ρ_0	−1.2281	−1.8731
ρ_1	4.1362×10^{-1}	2.9473×10^{-1}
ρ_2	5.6175×10^{-2}	4.7155×10^{-2}
ρ_{cl}	5.050	8.208
Pressure (/MPa)		
P_{c0}	5.795	3.629
P_0	1.1126×10^{-1}	−1.1105
P_1	4.6540×10^{-1}	0
P_{cl}	4.065	5.795

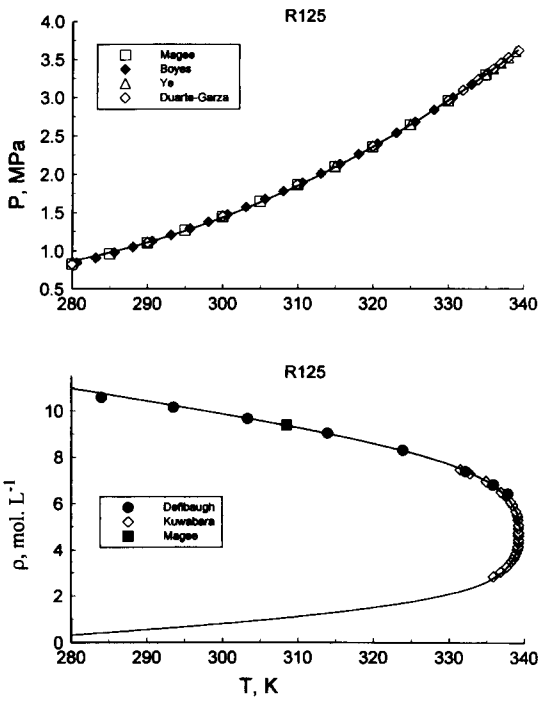

Figure 6 VLE data for R125 obtained by Magee[10], by Boyes and Weber[15], by Ye and co-workers[14], by Duarte-Garza and co-workers[12], by Defibaugh and Morrison[13] and by Kuwubara and co-workers[27], with predictions of the crossover equation of state

Figure 6 *Données VLE du R125 obtenues par Magee[10], par Boyes et Weber [15], par Ye et al.[14], par Duarte-Garza et al.[12], par Defigaugh et Morrison[13] et par Kuwubara et al.[27], avec prédictions de l'équation d'état étendue*

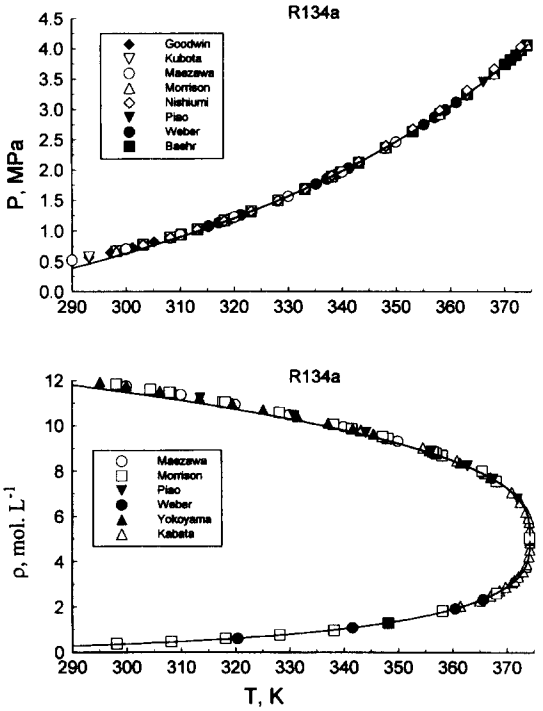

Figure 7 VLE data for R134a obtained by Goodwin and co-workers[28], by Kubota and co-workers[29], by Maezawa and co-workers[30], by Morrison and Ward[31], by Nishiumi and Yokoyama[32], by Piao and co-workers[20], by Weber[13], by Baehr and Tillner-Roth[33], by Yokoyama and Takahashi[34] and by Kabata and co-workers[35], with predictions of the crossover equation of state

Figure 7 *Donées VLE du R134a obtenues par Goodwin et al.[28], par Kubota et al.[29], par Maezawa et al.[30], par Morrison et Ward[31], par Nishiumi et Yokoyama[32], par Piao et al.[20], par Weber[13], par Baehr et Tillner-Roth[33], par Yokoyama et Takahashi[34] et par Kabata et al.[35], avec les prédictions de l'équation de l'état étendue*

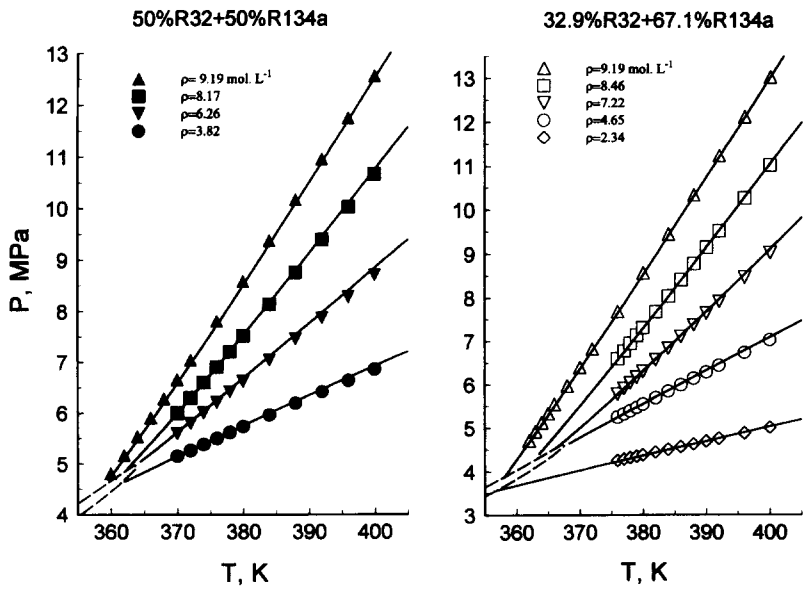

Figure 8 *PVT* data for R32 + R134a mixtures obtained by Magee[39] with predictions of the crossover equation of state

Figure 8 *Données PVT pour mélanges R32 + R134a, obtenues par Magee[39], avec prédictions de l'équation de l'état étendue*

R32 and R125. The resulting values for m_i are given in *Table 4*. In *Figure 4* we show a comparison of calculated and experimental sound speed for R134a. The data[24] were not used in the fit since they are on the edge or out of the range specified by eqn (19); however the agreement with the data is still good, and corresponds to that found by Sengers[7].

The parameters for the parametric crossover model given in *Table 4* were found using data in the one-phase region only. However, the parametric crossover model may be extrapolated to represent the thermodynamic surface at lower temperatures, as shown in *Figures 5–7*. These figures show good agreement between the model and experimental data[10,25–35] for vapor pressure, saturated liquid and saturated vapor density down to about 17–20% below the critical temperature. Since the parametric crossover model does not reproduce the ideal gas limit at low densities, and may even give unphysical behavior as $\rho \rightarrow 0$, we cannot extrapolate VLE calculations to temperatures below $0.8T_c$. However, even in the present form, the parametric crossover model reproduces experimental VLE data for R134a in the same temperature region as the renormalized Carnahan–Starling–DeSantis equation of van Pelt *et al.*[36].

Crossover free-energy model for binary mixtures

Once the pure fluid equations of state for the components of a binary mixture are known, only the critical locus of the binary mixture is needed in order to be able to predict the phase behavior of the mixture. It is not necessary to fit additional experimental data[1,2]. Unfortunately, we do not know the critical locus for either the R32 + R134a or R125 + R32 mixtures. Only two data points[37,38] on the T_c–x and ρ_c–x curves are available, and this is not enough information to determine all of the adjustable parameters required in eqns (11)–(13). Therefore we used empirical correlations proposed by Higashi[37,38] to generate T_c–x and ρ_c–x curves, and we fit this information to eqns (11) and (12) to obtain the coefficients ρ_i (i = 0,1,2) and T_i (i = 0,1,2). These values are listed in *Table 5*. Since there was no information about the critical pressure, we had to estimate the values of the parameters P_i (i = 0,1) in eqn (13) from a fit of eqns (5)–(18) to the experimental *PVTx* data[39] in the one-phase region. In addition, since for the R125 + R32 mixture, data for only one composition were available, we had to restrict eqn (12) for this mixture to $i = 0$. The resulting values of the P_i coefficients are given in *Table 5*.

Figures 8 and 9 compare the values obtained from our model with the *PVT*–x data of Magee[39]. The model shows good agreement for R32 + R134a mixtures, while for R125 + R32 mixtures along the isochore ρ = 8.360 mol L^{-1}, systematic deviations up to 5% are

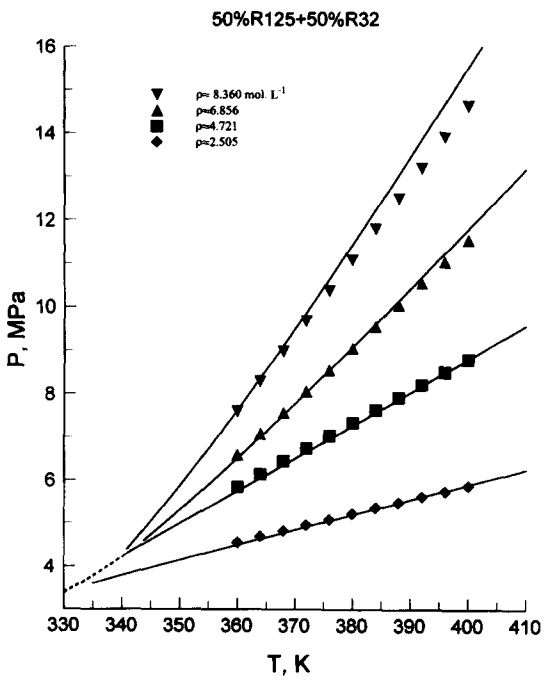

Figure 9 *PVT* data for R125 + R32 mixtures obtained by Magee[39] with predictions of the crossover equation of state

Figure 9 *Données PVT pour mélanges R125 + R32, obtenues par Magee[39], avec les prédictions de l'équation de l'état étendue*

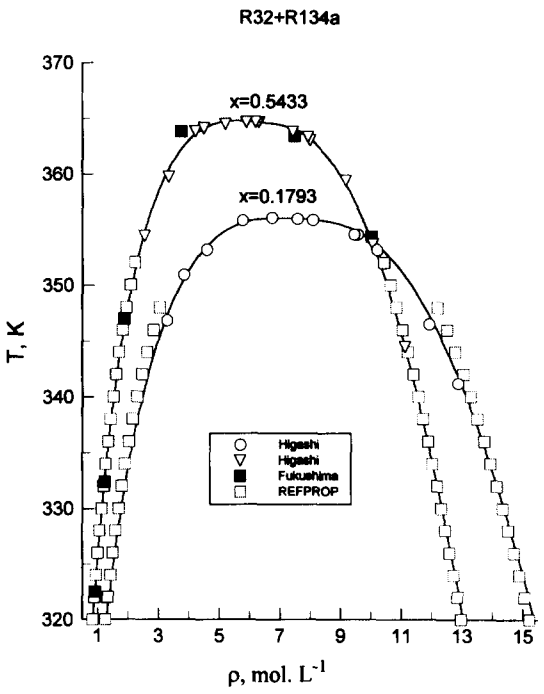

Figure 10 VLE data for R32 + R134a mixtures of Higashi[37] and of Fukushima[21] at two concentrations of R134a and predictions from the computer program NIST REFPROP[40] and of the crossover model (curves)

Figure 10 *Données VLE pour mélanges R32 + R134a de Higashi[37] et de Fukushima[21], à deux concentrations de R134a, et prédictions du logiciel NIST REFPROP et du mod èle étendu (courbes)*

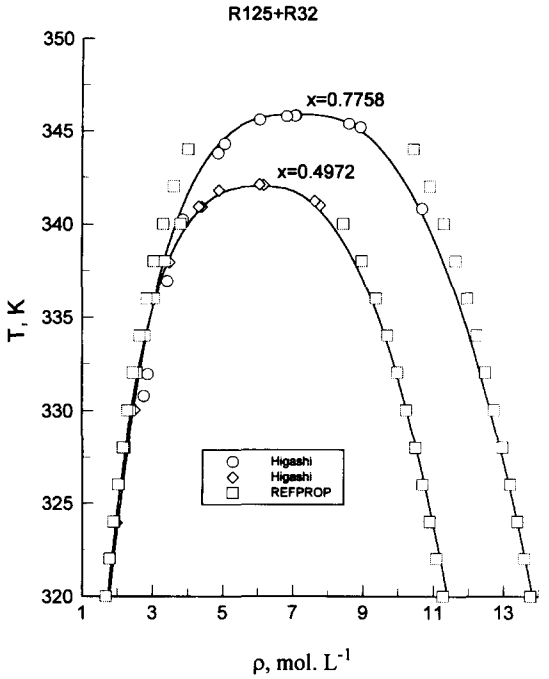

Figure 11 VLE data for R125 + R32 mixtures of Higashi[38] and at two concentrations of R32 and predictions from the computer program NIST REFPROP[40] and of the crossover model (curves)

Figure 11 *Données VLE de Higashi[38] pour mélanges R125 + R32 pour deux concentrations de R32, et prédictions de logiciel NIST REFPROP et du modèle étendu (courbes)*

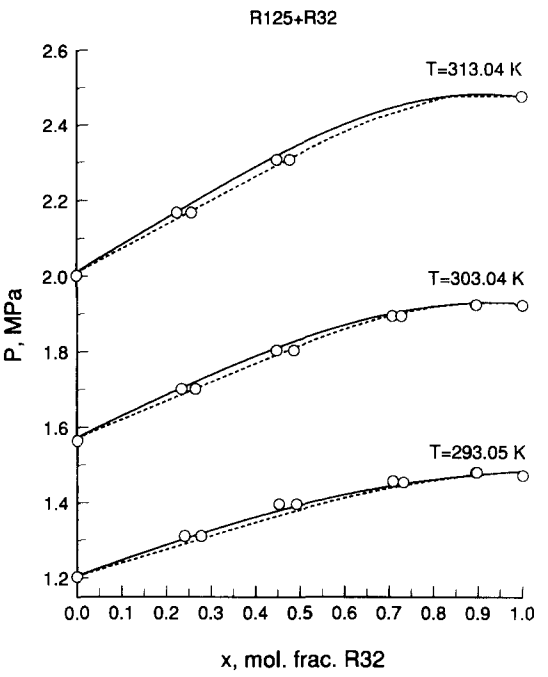

Figure 12 The pressure–composition diagram for R125 + R32 mixtures. The symbols indicate experimental data obtained by Higashi[38] at three temperatures, and the curves represent values calculated with the crossover model

Figure 12 *Diagramme pression-titre de mélanges R125 + R32. Les symboles indiquent les valeurs expérimentales obtenues par Higashi[38] pour trois températures, et les courbes représent les valeurs calculées avec le modèle étendu*

observed at temperatures $T > 370$ K. Since our crossover model contains not only the critical locus but also its derivatives (see eqn (14)), for a better description of the PVT–x surface of R125 + R32 mixtures a more accurate $P_c(x)$ line is needed.

Even though the parameters for P_i were found using one-phase data, the model can be extrapolated into the two-phase region down to about 10% below the critical temperature. *Figures 10 and 11* show the VLE coexistence curve for R32 + R134a and R125 + R32 mixtures in the critical region and below. The model agrees very well with the data of Higashi[37,38] in the critical region. For comparison, we also have shown the predictions from the computer program NIST REFPROP[40] which uses an extended corresponding states model that cannot be used in the near critical region, but that generally represents VLE for refrigerant mixtures well at lower temperatures. *Figure 12* shows the experimental VLE for R125 + R32 mixtures at four isotherms[38] and the predictions of our model. It is interesting to note that the model predicts the appearance of an azeotrope at approximately 90 mol% R32 at temperatures above 303 K. *Figure 13* shows a comparison of the calculated values of pressure with our crossover model, with an empirical equation of Kagawa[41], and with the experimental data of Higashi[42] in the two-phase region for R32 + R134a mixtures. Even though the equation of Kagawa[41] was obtained from a fit to experimental data in the two-phase region, our crossover model yields a better representation of these experimental data of Higashi[42] than the equation given by Kagawa [41].

In *Figure 14* we compare the predictions of the model for $PVTx$ properties for a 30 mass% R32 + 70 mass% R134a system (45.67 mol% R32 + 54.33 mol% R134a) with the experimental data of Fukushima *et al.*[43]. The data are over a wide range of temperatures from 314 K to 424 K and at pressures from 1.5 MPa to 10.1 MPa, and densities over the range $\rho = 0.902$ mol L^{-1} to $\rho = 10.033$ mol L^{-1}. The model shows good agreement with the data except at the lowest pressures. At the isochores $\rho = 0.902$ mol L^{-1} and $\rho = 1.236$ mol L^{-1}, which correspond to densities outside of the range specified by eqn (19), systematic deviation of the calculated values of pressure from the experimental data is observed. This deviation is a direct consequence of the fact that, as was mentioned above, our crossover model fails to reproduce the ideal gas limit.

We could not locate any experimental data for sound speed or specific heat for R32 + R134a mixtures in the critical region. Therefore, in *Figures 15 and 16* we compare the values calculated with our crossover model for sound velocity and specific heat along the dew-bubble curve for 30 mass% R32 + 70 mass% R134a mixtures (45.67 mol% R32 + 54.33 mol% R134a) with

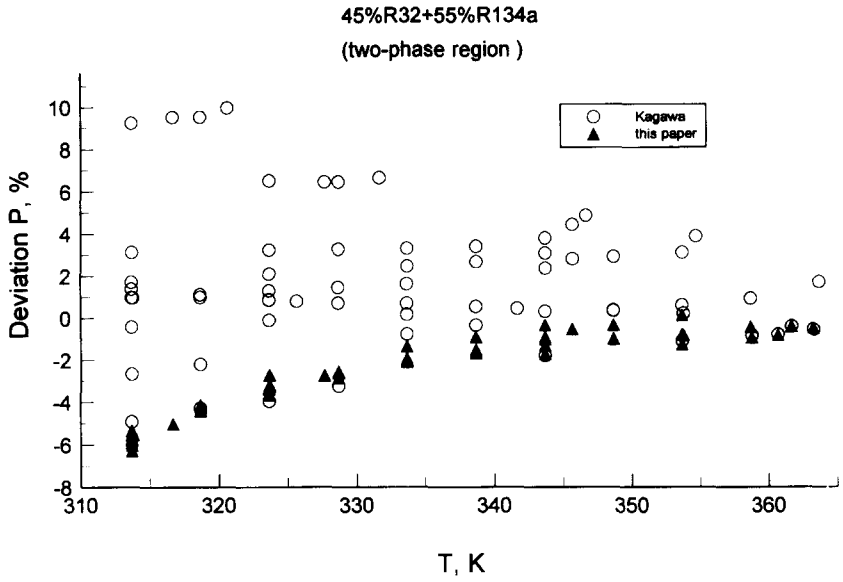

Figure 13 Percentage deviations of experimental pressures in the two-phase region for R32 + R134a mixtures obtained by Higashi[42] from values calculated with the empirical equation of Kagawa[41] (empty symbols) and with the crossover model (filled symbols)

Figure 13 *Déviations, en pourcentages, entre pressions expérimentales dans la région biphasique obtenues par Higashi*[42]*, et les valeurs calculées avec l'équation empirique de Kagawa*[41] *(symboles vides) et avec le modèle étendu (symboles pleins)*

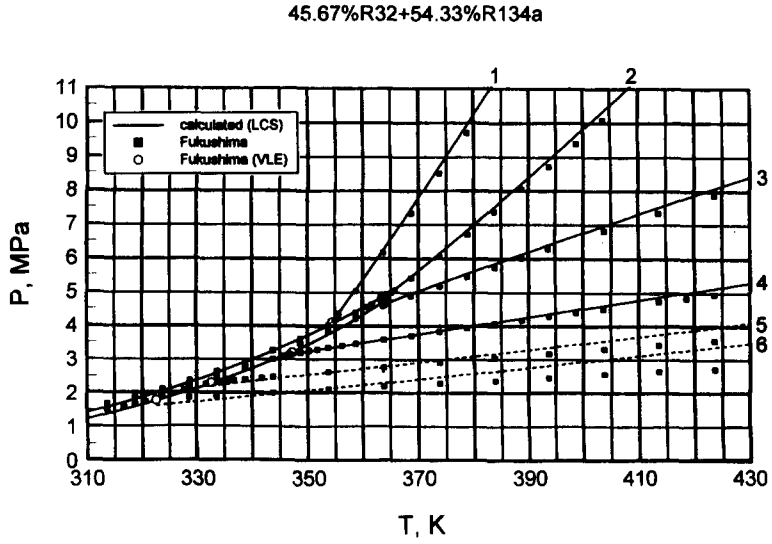

Figure 14 *PVT* data for R32 + R134a mixtures obtained by Fukushima and co-workers[43] with predictions of the crossover model: (1) $\rho = 10.033$ mol L^{-1}; (2) $\rho = 7.486$ mol L^{-1}; (3) $\rho = 3.743$ mol L^{-1}; (4) $\rho = 1.874$ mol L^{-1}; (5) $\rho = 1.236$ mol L^{-1}; (6) $\rho = 0.902$ mol L^{-1}

Figure 14 *Données PVT pour mélanges R32 + R134a obtenues par Fukushima et al.*[43] *et prédictions du modèle étendu*

values calculated with the 18-term modified Benedict–Webb–Rubin equation of state developed by Piao *et al.*[44] and with a mixture model developed by Lemmon[45]. Except for very low densities along the dew curve where our crossover model is not applicable, all equations give approximately the same results. In the near critical region, the analytical equations of Piao *et al.*[44] and of Lemmon[45] fail to reproduce singular behavior of the sound velocity and of the isochoric specific heat $C_{v,x}$ for R32 + R134a mixtures, and only the crossover model can be used.

Conclusions

We present a model for the thermodynamic properties of binary mixtures that has scaling-law behavior in the critical region and that crosses over to mean-field behavior away from critical conditions. In addition to

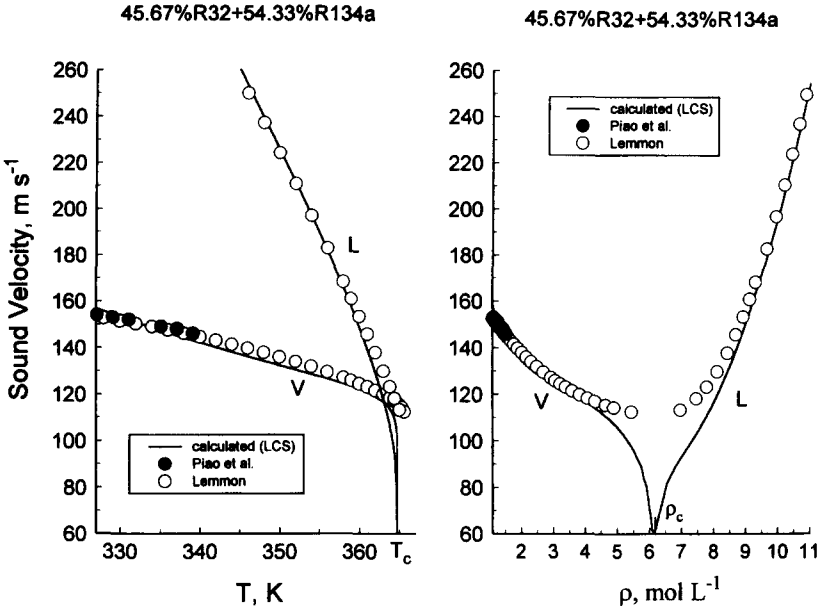

Figure 15 The sound-velocity of R32 + R134a mixtures at the dew-bubble curve at constant composition as a function of temperature (left) and density (right). The filled symbols indicate values calculated with the equation of Piao *et al.*[44], the empty symbols correspond to the values calculated with the equation of Lemmon[45], and the curves represent values calculated with the crossover model

Figure 15 *Vitesse du son dans les mélanges R32 + R134a sur la courbe de rosée-ébullition à composition constante en fonction de la température (à gauche) et de la densité (à droite). Les symboles pleins indiquent les valeurs calculées avec l'équation de Piao et al.*[44], *les symboles vides correspondent aux valeurs calculées avec l'équation de Lemmon*[45], *et les courbes représentent les valeurs calculées acev le modèle étendu*

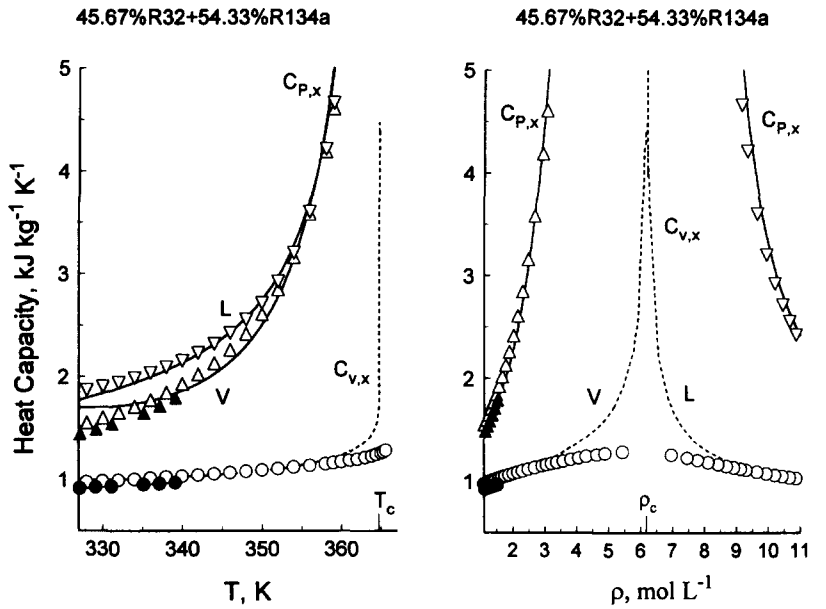

Figure 16 The isochoric specific heat $C_{v,x}$ and the isobaric specific heat $C_{P,x}$ of R32 + R134a mixtures at the dew-bubble curve at constant composition as a function of temperature (left) and density (right). The filled symbols indicate values calculated with the equation of Piao *et al.*[44], the empty symbols correspond to the values calculated with the equation of Lemmon[45], and the curves represent values calculated with the crossover model

Figure 16 *Chaleur massique isochore $C_{v,x}$ et chaleur massique isobare $C_{p,x}$ de mélanges R32 + R134a sur la courbe de rosée-ébullition à composition constante. en fonction de la température (à gauche) et de la densité (à droite). Les symboles pleins indiquent les valeurs calculées avec l'équation de Piao et al.*[44], *les symboles vides correspondent aux valeurs calculées avec l'équation de Lemmon*[45], *et les courbes représentent les valeurs calculées avec le modèle étendu*

the pure fluid parameters, the model requires only that the critical locus for the binary mixture be known. All other mixture parameters are obtained from generalized corresponding states relations developed in a earlier work using methane and ethane[2]. The model can be applied to predict all thermodynamic one-phase and two-phase behavior including PVTx and VLE behavior, in a region around the critical point. We have applied this model to

two refrigerant mixtures, R32 + R134a and R125 + R32 and have shown excellent agreement with both *PVTx* and VLE experimental data in the range of applicability given by eqn (19). The model can be extrapolated to a wider range of temperatures, down to about 20% below the critical temperature, and still give qualitatively correct behavior. In order to extend our approach to the entire thermodynamic surface including the ideal gas limit, a crossover cubic equation of state can be used, but so far it has been applied only to pure fluids[36,46].

Acknowledgements

The authors are indebted to N. Kagawa, J.W. Magee and J.C. Rainwater for valuable discussions and constructive comments. We are also indebted to N. Kagawa for comparing our model with his equation and experimental data in the two-phase region for R32 + R134a mixture, and to J.W. Magee for providing us with experimental data prior to publication. One of us (S.B.K.) also would like to thank the Physical and Chemical Properties Division, National Institute of Standards and Technology for the opportunity to work as a Guest Researcher at NIST during the course of this research.

Appendix A Relevant thermodynamic quantities

Pressure P and its derivatives,

$$\frac{P(\rho,T,\tilde{x})}{R\rho_{c0}T_{c0}}=\frac{\rho}{\rho_c}\left(\frac{\partial\Delta\tilde{A}}{\partial\Delta\rho}\right)_{\tau,\tilde{x}}-\Delta\tilde{A}-\tilde{A}_0, \tag{A1}$$

$$\left(\frac{\partial P}{\partial T}\right)_{\rho,x}=\left(\frac{\partial P}{\partial T}\right)_{\rho,\tilde{x}}+\left(\frac{\partial P}{\partial\tilde{x}}\right)_{\rho,T}\left(\frac{\partial\tilde{x}}{\partial T}\right)_{\rho,x}, \tag{A2}$$

$$\left(\frac{\partial P}{\partial\rho}\right)_{T,x}=\left(\frac{\partial P}{\partial\rho}\right)_{T,\tilde{x}}+\left(\frac{\partial P}{\partial\tilde{x}}\right)_{T,\rho}\left(\frac{\partial\tilde{x}}{\partial\rho}\right)_{T,x}, \tag{A3}$$

$$\left(\frac{\partial P}{\partial x}\right)_{T,\rho}=\left(\frac{\partial P}{\partial\tilde{x}}\right)_{T,\rho}\left(\frac{\partial\tilde{x}}{\partial x}\right)_{T,\rho}, \tag{A4}$$

where the critical part,

$$\Delta\tilde{A}(\tau,\Delta\rho,\tilde{x})=\tilde{k}r^{2-\alpha}R^{\alpha}(q)\times\left[\tilde{a}\Psi_0(\theta)+\sum_{i=1}^{4}\tilde{c}_i r^{\Delta_i}R^{-\tilde{\Delta}_i}(q)\Psi_i(\theta)\right], \tag{A5}$$

and background contribution,

$$\tilde{A}_0(T,\tilde{x})=\sum_{i=1}^{4}\tilde{A}_i\tau^i(\tilde{x})-\frac{P_c(\tilde{x})}{R\rho_{c0}T_{c0}}. \tag{A6}$$

Isochoric specific heat capacity $C_{v,x}$,

$$\frac{\rho C_{v,x}(T,\rho,\tilde{x})}{TR\rho_{c0}T_{c0}}=-\left(\frac{\partial^2\Delta\tilde{A}}{\partial T^2}\right)_{\rho,\tilde{x}}-\left(\frac{\partial^2\tilde{A}_0}{\partial T^2}\right)_{\tilde{x}}-\frac{\rho}{\rho_{c0}}\left(\frac{\partial^2\tilde{M}_0}{\partial T^2}\right)_{\tilde{x}}-\left[\left(\frac{\partial^2\Delta\tilde{A}}{\partial T\partial\tilde{x}}\right)+\left(\frac{\partial^2\tilde{A}_0}{\partial T\partial\tilde{x}}\right)+\frac{\rho}{\rho_c}\left(\frac{\partial^2\tilde{M}_0}{\partial T\partial\tilde{x}}\right)\right]\left(\frac{\partial\tilde{x}}{\partial T}\right)_{\rho,x} \tag{A7}$$

with

$$\tilde{M}_0(T,\tilde{x})=\sum_{i=1}^{4}\tilde{m}_i\tau^i(\tilde{x})+\frac{\rho_c T}{\rho_{c0}T_{c0}}[\ln(1-\tilde{x})+\tilde{m}_0]. \tag{A8}$$

Isobaric specific heat capacity $C_{P,x}$,

$$C_{P,x}(T,\rho,\tilde{x})=C_{v,x}(T,\rho,\tilde{x})+T\left(\frac{\partial P}{\partial T}\right)^2_{\rho,x}\left(\frac{\partial P}{\partial\rho}\right)^{-1}_{T,x}\rho^{-2} \tag{A9}$$

Sound-velocity w_s,

$$w_s(T,\rho,\tilde{x})=\left[\left(\frac{\partial P}{\partial\rho}\right)_{T,x}\frac{C_{P,x}}{C_{v,x}}\right]^{1/2}. \tag{A10}$$

The derivatives,

$$\left(\frac{\partial\tilde{x}}{\partial T}\right)_{\rho,x}=-\left(\frac{\partial x}{\partial T}\right)_{\rho,\tilde{x}}\left(\frac{\partial\tilde{x}}{\partial x}\right)_{\rho,T}, \tag{A11}$$

$$\left(\frac{\partial\tilde{x}}{\partial\rho}\right)_{T,x}=-\left(\frac{\partial x}{\partial\rho}\right)_{T,\tilde{x}}\left(\frac{\partial\tilde{x}}{\partial x}\right)_{\rho,T}, \tag{A12}$$

where the derivatives $\left(\frac{\partial x}{\partial T}\right)_{\rho,\tilde{x}}$, $\left(\frac{\partial x}{\partial\rho}\right)_{T,\tilde{x}}$, and $\left(\frac{\partial\tilde{x}}{\partial x}\right)_{\rho,T}$ can be obtained analytically from the equation,

$$x=\tilde{x}-\tilde{x}(1-\tilde{x})\frac{\rho_{c0}T_{c0}}{\rho T}\times\left[\left(\frac{\partial\Delta\tilde{A}}{\partial\tilde{x}}\right)_{\rho,T}+\left(\frac{\partial\tilde{A}_0}{\partial\tilde{x}}\right)_T+\frac{\rho}{\rho_c}\left(\frac{\partial\Delta\tilde{M}_0}{\partial\tilde{x}}\right)_T\right], \tag{A13}$$

(here $\Delta\tilde{M}_0=\tilde{M}_0-(\rho_c T/\rho_{c0}T_{c0})\ln(1-\tilde{x})$), which provides a relationship between concentration x and the isomorphic variable $\tilde{x}$ at fixed temperature T and density ρ.

References

1. **Kiselev, S. B.,** *Fluid Phase Equilibria, 1997,* **128**, 1.
2. **Kiselev, S. B. and Rainwater, J. C.** Fluid Phase Equilibria, in press.
3. **Kiselev, S. B. and Kulikov, V. D.,** *Int. J. Thermophys., 1997,* **18**, 1143.
4. **Leung, S. S. and Griffiths, R. B.,** *Phys. Rev. A, 1973,* **8**, 2673.
5. **Kiselev, S. B. and Sengers, J. V.,** *Int. J. Thermophys., 1993,* **14**, 1.
6. **Outcalt, S. L. and McLinden, M. O.,** *Int. J. Thermophys., 1995,* **16**, 79.
7. **Luettmer-Strathmann, J. and Sengers, J. V.,** *High Temp.–High Press., 1994,* **26**, 673.
8. **Holste, J. C., Duarte-Garza, H. A. and Villamanan-Olfos, M. A.** Paper No. 93-WA/HT-60, ASME Winter Annual Meeting, New Orleans, December, 1993.
9. **Defibaugh, D. R., Morrison, G. and Weber, L. A.,** *J. Chem. Eng. Data, 1994,* **39**, 333.
10. **Magee, J. W.,** *Int. J. Thermophys., 1996,* **17**, 803.
11. **Malbrunot, P. F., Meunier, P. A., Scatena, G. M., Mears, W. H., Murphy, K. P. and Sinka, J. V.,** *J. Chem. Eng. Data, 1968,* **13**, 16.
12. **Duarte-Garza, H. A., Stouffer, C. E., Hall, K. R., Holste, J. C., Marsh, K. N. and Gammon, B. E.** submitted to *J. Chem. Eng. Data,* 1997.
13. **Defibaugh, D. R. and Morrison, G.,** *Fluid Phase Equilibria, 1992,* **80**, 157.
14. **Ye, F., Sato, H. and Watanabe, K.,** *J. Chem. Eng. Data, 1995,* **40**, 148.

15. **Boyes, S. J. and Weber, L. A.,** *J. Chem. Thermodynamics, 1995,* **27**, 163.
16. **Wilson, L. C., Wilding, W. V., Wilson, G. M., Rowley, R. L., Felix, V. M. and Chisolm-Carter, T.,** *Fluid Phase Equilibria, 1992,* **80**, 167.
17. **Tillner-Roth, R. and Baehr, H. D.,** *J. Chem. Thermodynamics, 1992,* **24**, 413.
18. **Weber, L. A.,** *Int. J. Thermophys., 1989,* **10**, 617.
19. **Wilson, D. P. and Basu, R. S.,** *ASHRAE Trans., 1988,* **94**, 2095.
20. **Piao, C. C., Sato, H. and Watanabe, K.,** *ASHRAE Trans., 1990,* **96**, 132.
21. **Fukushima, M.,** *Trans. Jpn. Assoc. Refrig., 1990,* **7**, 243.
22. **Krauss, R., Luettmer-Strathmann, J., Sengers, J. V. and Stephan, K.,** *Int. J. Thermophys., 1993,* **14**, 951.
23. **Huber, M. L. and Ely, J. F.,** *Int. J. Refrigeration, 1994,* **17**, 18.
24. **Guedes, H. J. R. and Zollweg, J. A.,** *Int. J. Refrig., 1992,* **15**, 381.
25. **Holcomb, C. D., Niesen, V. G., VanPoolen, L. J. and Outcalt, S. L.,** *Fluid Phase Equilibria, 1993,* **91**, 145.
26. **Higashi, Y.,** *Int. J. Refrigeration, 1994,* **17**, 524.
27. **Kuwubara, S., Aoyama, H., Sato, H. and Watanabe, K.,** *J. Chem. Eng. Data, 1995,* **40**, 112.
28. **Goodwin, A. R. H., Defibaugh, D. R. and Weber, L. A.,** *Int. J. Thermophys., 1993,* **13**, 837.
29. **Kubota, H., Yamashita, T., Tanaka, Y. and Makita, T.,** *Int. J. Thermophys., 1989,* **10**, 629.
30. **Maezawa, Y., Sato, H. and Watanabe, K.,** *J. Chem. Eng. Data, 1990,* **35**, 225.
31. **Morrison, G. and Ward, D. K.,** *Fluid Phase Equilibria, 1991,* **62**, 65.
32. **Nishiumi, H. and Yokoyama, T.** Proc. 11th Japan Symp. Thermophysical Prop., Paper B105, 1990.
33. **Baehr, H. D. and Tillner-Roth, R.,** *J. Chem. Thermodynamics, 1991,* **23**, 1063.
34. **Yokoyama, C. and Takahashi, S.,** *Fluid Phase Equilibria, 1991,* **67**, 227.
35. **Kabata, Y., Tanikawa, S., Uematsu, M. and Watanabe, K.,** *Int. J. Thermophys., 1989,* **10**, 605.
36. **van Pelt, A., Jin, G. X. and Sengers, J. V.,** *Int. J. Thermophys., 1994,* **15**, 687.
37. **Higashi, Y.,** *Int. J. Thermophys., 1995,* **16**, 1175.
38. **Higashi, Y.** In *19th International Congress Refrigeration 1995, Proceedings*, Volume IVa, pp. 297–305.
39. **Magee, J. W.** Div. 838.08, NIST, Boulder, CO, personal communication, 1997.
40. NIST Thermodynamic Properties of Refrigerant Mixtures Database, NIST REFPROP, v5.12, Natl. Inst. Stand. Technol., Gaitherburg, MD, 1997.
41. **Kagawa, N.** Presented at the 12th Symposium on Thermophysical Prop., Boulder, CO, U.S.A., 19–24 June 1994.
42. **Higashi, Y.** Presented at the 12th Symposium on Thermophysical Prop., Boulder, CO, U.S.A., 19–24 June 1994.
43. **Fukushima, M., Machidori, K., Kumano, S. and Ohotoshi, S.** In *Proc. 14th Japan Symp. Thermophysical Properties*, 275, 1993.
44. **Piao, C.-C., Iwata, I., Fujiwara, K. and Noguchi, M.** In *Proc. of the 19th Int. Congress of Refrigeration*, The Hague, The Netherlands, 20–25 August 1995, IVa, pp. 488–495.
45. **Lemmon, E. W.** A generalized model for the prediction of the thermodynamic properties of mixtures including vapor–liquid equilibrium. Ph.D. Dissertation, University of Idaho, Moscow, 1996.
46. **Kiselev, S. B.** Fluid Phase Equilibria. 1998, in press.